Geomechanics and Engineering, *Vol. 30, No. 3 (2022) 233-246*
https://doi.org/10.12989/gae.2022.30.3.233

PGA estimates for deep soils atop deep geological sediments -An example of Osijek, Croatia

Borko Đ. Bulajić*[1], Marijana Hadzima-Nyarko[2a] and Gordana Pavić[2b]

[1]*Faculty of Technical Sciences, University of Novi Sad, Trg Dositeja Obradovića 6, 21000 Novi Sad, Serbia*
[2]*Faculty of Civil Engineering and Architecture Osijek, Josip Juraj Strossmayer University of Osijek, Vladimira Preloga 3, 31000 Osijek, Croatia*

(*Received July 20, 2021, Revised April 15, 2022, Accepted June 30, 2022*)

Abstract. In this study, the city of Osijek is used as a case study area for low to medium seismicity regions with deep soil over deep geological deposits to determine horizontal PGA values. For this reason, we propose new regional attenuation equations for PGA that can simultaneously capture the effects of deep geology and local soil conditions. A micro-zoning map for the city of Osijek is constructed using the derived empirical scaling equations and compared to all prior seismic hazard estimates for the same area. The findings suggest that the deep soil atop deep geological sediments results in PGA values that are only 6 percent larger than those reported at rock soil sites atop geological rocks. Given the rarity of ground motion records for deep soils atop deep geological layers around the world, we believe this case study is a start toward defining more reliable PGA estimates for similar areas.

Keywords: deep geological sediments; deep soil; horizontal; microzoning; PGA

1. Introduction

Most empirical equations for scaling peak ground acceleration (hereinafter, PGA) values only consider the impacts of local soil and ignore the effects of deep geological site surroundings (Douglas 2003). However, several strong motion studies have demonstrated that, to avoid bias, when estimating the severity of surface ground motion, both the deep geology and the local soil conditions must be simultaneously considered (Lee 1987, Trifunac 1990, Bulajić *et al.* 2013, 2018). The 2004 version of Eurocode 8 (EN 1998-1:2004 2004) also recognizes the importance of deeper geological conditions by stating in Clause 3.1.2(1) that the National Annex may specify the classification scheme that will account for the deep geology. Here, the term "deep geology" refers to geological settings on the scale of a few kilometers or at least hundreds of meters (Trifunac and Brady 1975), whereas "local soil" refers to geotechnical site description on the scale of a few tens of meters, usually down to the first soil layers with the average shear wave velocity, $V_S \geq 800$ m/s.

Furthermore, most Ground Motion Prediction Equations (hereinafter, GMPEs) classify local soil conditions by just considering the top 30 m of the stratigraphic profile, despite research showing that the average shear-wave velocity of the top 20 or 30 m does not correspond with site resonance (Peng *et al.* 2020, Tavakoli *et al.* 2016), especially not for the deep soil sites (Jakka *et al.* 2015). This method is still widely used because data on deep geology is scarce and investigating the soil profile to depths of 100 or 200 m would be prohibitively expensive for civil engineering design.

In Croatia, seismic hazard maps created for use in the scope of Eurocode 8 (EN 1998-1:2004 2004) are defined for ground type A, which is defined as rock or "other rock-like geological formation" with up to 5 m of weaker surface material and with V_S>800 m/s in the top 30 m of the soil profile. The PGA at the surface of a local soil is then calculated by multiplying the PGA value obtained from the official hazard map by the so-called *soil factor*, *S*. Table 1 shows how *S* varies with the ground type. *S* also depends on the type of spectrum-Type 1 or Type 2-which is determined by the magnitude of the "most contributing earthquakes" (EN 1998-1:2004 2004). Table 1 demonstrates that *S* is greater than 1 for all ground types (except for the normative type A) and both spectrum types, implying that ground motion will be amplified relative to the rock sites. However, the empirical attenuation equations developed in the mid-1980s for California based on 1482 acceleration components from earthquakes in the western United States indicate a 30% de-amplification of PGA values in deep soils (Lee 1987, Lee and Trifunac 2010). This de-amplification would result in *S* equal to 0.70 in Eurocode 8 terminology.

The primary goal of this study is to estimate PGA values at deep soil sites atop deep geological deposits. The case-study region encompasses the entire city of Osijek, Croatia, for which our associated studies (Bulajić *et al.* 2021a, b, 2022) examined vertical PGA values as well as uniform hazard spectral estimates. Osijek is located in the south-central part of the Pannonian basin, along the Danube River and the Drava River, in a region with less seismic activity

*Corresponding author, Associate Professor
E-mail: borkobulajic@uns.ac.rs
[a]Associate Professor
E-mail: mhadzima@gfos.hr
[b]Ph.D. Student
E-mail: gordana.pavic2@gmail.com

ISSN: 2005-307X (Print), 2092-6219 (Online)

Table 1 PGA estimates for various ground types according to Eurocode 8 (EN 1998-1:2004 2004), where a_g signifies the PGA value shown on the associated seismic hazard map for the examined site

Eurocode 8 (EN 1998-1:2004 2004) ground types	Type 1 Spectrum: "most contributing" earthquakes with M_S>5.5	Type 2 Spectrum: "most contributing" earthquakes with M_S≤5.5
Ground Type A, $V_{S,30}$>800 m/s Rock, at the surface up to 5 m of weaker material.	a_g	a_g
Ground Type B, $V_{S,30}$=360-800 m/s At least several tens of meters thick deposits. Very dense sand, gravel, or very stiff clay.	a_g×1.2	a_g×1.35
Ground Type C, $V_{S,30}$=180-360 m/s Deep deposits, several tens of meters up to hundreds of meters thick. Dense or medium dense sand, gravel, or stiff clay.	a_g×1.15	a_g×1.5
Ground Type D, $V_{S,30}$<180 m/s Deposits. Loose-to-medium cohesionless soil, or predominantly soft-to-firm cohesive soil.	a_g×1.35	a_g×1.8
Ground Type E Alluvium layer at the surface, between 5 and 20 m thick, above stiffer material. $V_{S,30}$<360 m/s.	a_g×1.4	a_g×1.6

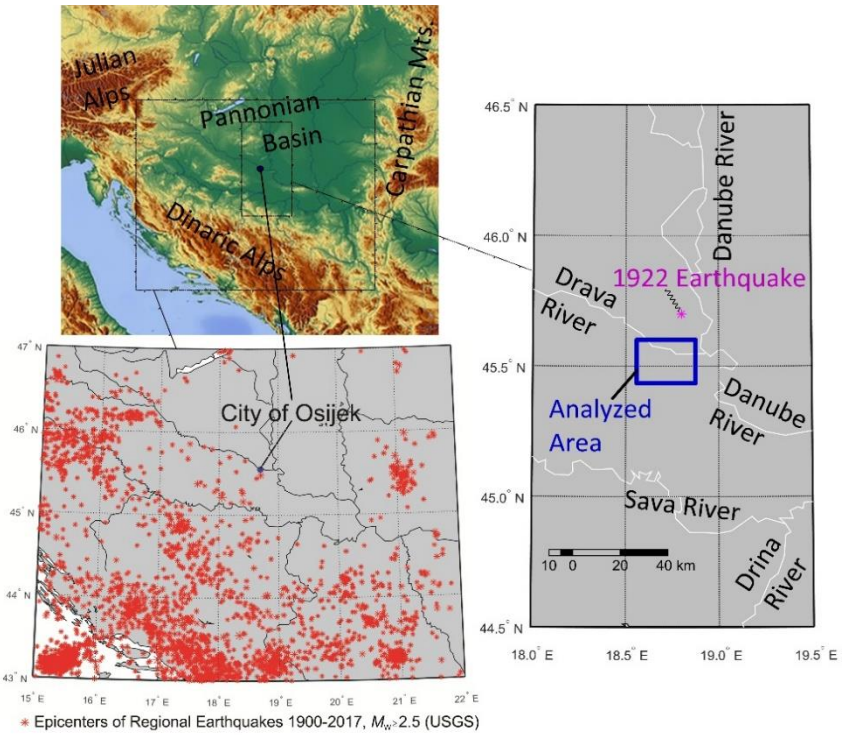

Fig. 1 The location of the investigated area inside the Pannonian Basin and the epicenters of regional earthquakes in the period between 1900 and 2017 (USGS 2017)

than other parts of Croatia and the North-Western Balkans, as seen in Fig. 1.

We will generate seismic hazard maps for the examined area using new GMPEs for PGA and compare the results to existing PGA and macroseismic intensity estimates. In this study, the local soil classification will be based on the one proposed by Seed *et al.* (1976a, b). This classification will be the same as that specified for the accelerograph locations in former Yugoslavia by Trifunac *et al.* (1991), Lee and Trifunac (1993), and Lee and Manić (1994). The "rock" soil locations will be the ones with V_S>800 m/s. The stiff soil sites will have a 15 to 75 m thick soil layer atop the "rock" layer, while the deep soil sites will have a soil layer that is more than 100 m thick. For deep geology, we will use Trifunac and Brady's (1975) classification, which divides deep geology into three categories: the basement rock, (deep geological) sediments, and (complex or) intermediate sites. To minimize confusion with the varieties of local soil, we will further use "geological rock" rather than the "basement rock."

2. The case-study area-seismicity and site conditions

2.1 Seismicity of the analyzed area

The city of Osijek is located in the south-central part of the Pannonian Basin, which is an intraplate seismicity

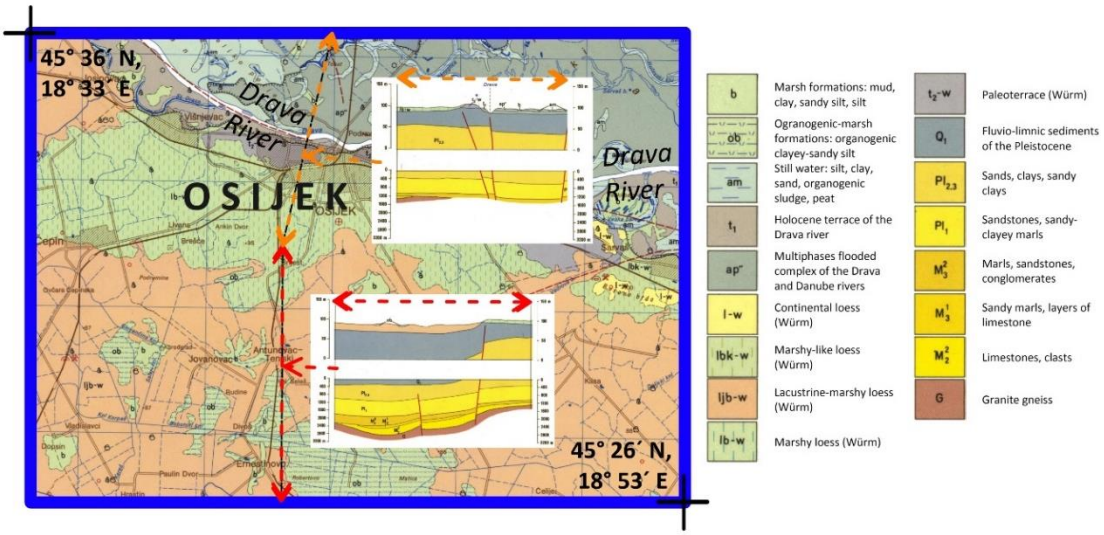

Fig. 2 Two typical geotechnical profiles and the geological map for the analyzed region (Magaš *et al.* 1987)

region, with a rare occurrence of larger events (Morales-Esteban *et al.* 2014, 2021). Due to the collision of the Adriatic Platform and the Dinarides, the majority of earthquakes in Croatia occur around the Adriatic coast (see Fig. 1 in Bulajić *et al.* 2021a). In the western Balkans, Moho depth increases from 25 km beneath the Pannonian Basin to 45 km beneath the Dinarides (Skoko *et al.* 1987, Bielik *et al.* 2018).

The epicenter locations of regional earthquakes with $M_w \geq 2.5$ that were observed between 1900 and 2017, as reported by the US Geological Survey (USGS 2017), are shown in Fig. 1. The closest seismic source zones to the examined area are Bansko Brdo, 30 km away, and Dilj Gora, 70 km away. On November 24, 1922, the strongest historical earthquake in the vicinity of Osijek occurred as part of the 1922-1924 seismic activity, with an epicenter 20 km north of the city (see the right plot in Fig. 1) and a hypocentral depth of 18 km. According to the SHARE European Earthquake Catalogue (Stucchi *et al.* 2013), the magnitude was M_L=4.9 while by the UNESCO catalog from 1974 (UNESCO 1974), the magnitude was estimated to be 5.1. The intensity in the epicentral region was VII-VIII (°MCS). In Osijek, the intensity was VII (°MCS).

Osijek is the fourth largest city in Croatia, with a population of 108,000 inhabitants. Recent seismic risk studies reveal a substantial number of older buildings built before 1964 and the first earthquake-resistant design codes in former Yugoslavia (Pavić *et al.* 2020a). Similar structures exist in other parts of Croatia and other Mediterranean countries and might sustain significant damage during earthquakes similar to the one that struck near Osijek in 1922 (Inel *et al.* 2008, Kaplan *et al.* 2010, Bilgin *et al.* 2012, 2018, Işık *et al.* 2016, 2020, Pavić *et al.* 2020b). A destructive earthquake with M_L=5.5 (M_w=5.3) struck Zagreb, Croatia's capital, on March 22, 2020, with the epicenter 7 km north of the city center (EMSC-CSEM 2021) and a focal depth of 10 km. This was the strongest earthquake near Croatia's capital since the 1880 Zagreb earthquake with M_w=6.3 (Prelogović and Cvijanović 1981). Another destructive earthquake struck Croatia on December 29, 2020, this time 40 km south of Zagreb and with a magnitude of 6.4. (Ganas *et al.* 2021). The 2020 Zagreb earthquake had a maximum felt intensity of VII (on the Modified Mercalli scale), causing substantial damage in the historic city center, with over 1,900 buildings reportedly becoming uninhabitable because of the destruction. There was a total of 27 persons hurt, one of them died as a result of the injuries. The earthquake that struck Zagreb in 2020 was also felt in Slovenia. Interestingly, even though the 1880 earthquake was believed to be stronger (maximum felt intensity VIII-IX) than the 2020 one and the population within today's city limits increased tenfold (from 80,000 to 800,000), the effects of the 1880 event were strikingly similar-around 1,800 buildings were damaged, 29 people were seriously injured, and one person succumbed to injuries.

2.2 Geological settings for the case-study area

The Pannonian basin (also known as the Carpathian basin) is located between the Julian Alps, Dinaric Alps, and the Carpathian Mountains in southeastern Central Europe (see Fig. 1). The basin encompasses parts of nine different countries, including northeast Croatia.

When the Pannonian Sea dried up (after its greatest geographical extent during the Pliocene), the basin's lowlands formed the plain that remained. The basin is a sediment-filled back-arc basin that spread apart during the Miocene (Balázs *et al.* 2016). There are numerous rivers and lakes within the basin, which is roughly divided in half by the Danube and Tisza rivers.

The Pannonian basin's deep geological strata date back to the time of the Pannonian Sea and are up to several kilometers thick (Timkó *et al.* 2019). The city of Osijek, as well as its surrounding area, is built over these deep geological layers. A rare exception can be seen 30 km north of the city, on Bansko Brdo hill, which is the sole hill in the vicinity, stretching 20 km NE-SW and including scattered outcrops of geological rocks (basalt-andesite and pyroclastic).

Table 2 Macroseismic intensity degrees from the seismic zoning maps of 1950 (Official Gazette of SFRY 1964), 1982 (Official Gazette of SFRY 1982), and 1990 (Official Gazette of SFRY 1990) for the five cities in Croatia, as well as the corresponding empirical PGA values, determined using Eq. (1)

City	Measure	1950	1982	1990					
				50 yrs.	100 yrs.	200 yrs.	500 yrs.	1000 yrs.	10,000 yrs.
Zagreb	*I* [°MCS]	VIII-IX	VIII	VII	VII-VIII	VIII	VIII-IX	IX	IX
	PGA [*g*]	0.159-0.388	0.159-0.199	0.081-0.102	0.081-0.199	0.159-0.199	0.159-0.388	0.309-0.388	0.309-0.388
Rijeka	*I* [°MCS]	IX	VII	VI	VII-VIII	VIII	VIII	VIII-IX	IX
	PGA [*g*]	0.309-0.388	0.081-0.102	0.042-0.052	0.081-0.199	0.159-0.199	0.159-0.199	0.159-0.388	0.309-0.388
Split	*I* [°MCS]	VII	VI	VII	VII	VII	VIII	VIII	VIII
	PGA [*g*]	0.081-0.102	0.042-0.052	0.081-0.102	0.081-0.102	0.081-0.102	0.159-0.199	0.159-0.199	0.159-0.199
Osijek	*I* [°MCS]	**VIII**	**VII**	**VI**	**VII**	**VII**	**VIII**	**VIII**	**VIII**
	PGA [*g*]	**0.159-0.199**	**0.081-0.102**	**0.042-0.052**	**0.081-0.102**	**0.081-0.102**	**0.159-0.199**	**0.159-0.199**	**0.159-0.199**
Zadar	*I* [°MCS]	IX	VIII	VI	VII	VII	VIII	VIII	VIII
	PGA [*g*]	0.309-0.388	0.159-0.199	0.042-0.052	0.081-0.102	0.081-0.102	0.159-0.199	0.159-0.199	0.159-0.199

The subsurface geology underlying the investigated region of Osijek (see the blue rectangle in Fig. 1) is made up of a complex of marls, sandstones, conglomerates, and limestones. These geological deposits have thicknesses of up to 3,000 m.

The Pannonian plain is also known for its loamy loess soil and is a significant agricultural area in Europe. The deep soil sites may be found along practically all rivers. The thickest loess sections (more than 50 m) in Croatia are found around the Danube River in the eastern part of the country (Banak *et al*. 2016).

Osijek is situated on the right bank of the Drava River, only 25 km upstream from its confluence with the Danube River (see the right plot in Fig. 1). As a result, the shallow geological formations are made up of loosely, muddy, and sandy soil with high groundwater levels. The Quaternary deposits in the investigated area (see Fig. 2) have a total thickness of 150-180 m (Pikija and Šikić 1991, Magaš *et al.* 1987). V_S ranges between 180 and 360 m/s in the top 30 m of the stratigraphic profiles, while layers with a velocity greater than 800 m/s are found at depths of more than 100 m. The local soil can be classified as deep soil according to categorization by Seed *et al.* (1976a, b). In addition, according to Eurocode 8 (EN 1998-1:2004 2004), the local soil might be categorized as Ground Type C (see Table 1).

2.3 Previous and current design PGA estimates

In 1964, ex-SFRY introduced its first code for seismic-resistant design (Official Gazette of SFRY 1964). There was a Seismic Zoning Map, created in 1950 based on the highest macro-seismic intensities observed at the time, and was used together with the 1964 code. In 1981, a new earthquake-resistant design code was enacted, and a year later (Official Gazette of SFRY 1982), a seismic zoning map was prepared to be temporarily utilized with the new code. The 1982 map was based on the highest observed intensities once again.

Finally, in 1990, the 1981 code was updated to include a set of six new seismic zoning maps (for return periods of 50, 100, 200, 500, 1000, and 10,000 years) (Official Gazette of SFRY 1990). Although the seismic hazard was expressed in seismic intensity degrees and for average soil conditions, they were the first seismic hazard maps in this region generated using the Probabilistic Seismic Hazard Assessment (hereinafter, PSHA) approach.

Table 2 shows macroseismic intensities for Croatia's five most populated cities, based on hazard maps from 1950, 1982, and 1990. Table 2 also includes the empirical PGA estimates, which were calculated using the following relationship (Trifunac *et al*. 1991)

$$\log(\text{PGAhoriz}) = -0.079 \cdot I + 0.290 \pm P \cdot \sigma,\ \sigma = 0.049 \quad (1)$$

where PGAhoriz [cm/s^2] is the PGA in the horizontal direction, I [°MCS] is the macroseismic intensity, and σ is the standard deviation, while P=0 for the median estimate. Table 2 displays the empirical PGA estimates for a median $-\sigma$ and median $+\sigma$ for each city.

In 2011, two new hazard maps were introduced in the Croatian National Annex to standard EN 1998-1 (HRN EN 1998-1:2011/NA 2011). In these two maps, seismic hazard is numerically expressed by the PGA values. The maps were created using the PSHA methodology. The first map is for a return period of 95 years, i.e., for the 10% in 10 years likelihood of exceedance, while the second is for a return period of 475 years, i.e., for the 10% in 50 years probability. The 95-year map corresponds to Eurocode 8 "damage limitation" requirement, while the 475-year map corresponds to Eurocode 8 "no-collapse" requirement (EN 1998-1:2004 2004). Both maps were created for ground type A, i.e., rock sites (see Table 1). Moreover, both maps ignore the impacts of the deep geology on surface ground motion.

The horizontal PGA values in Osijek, according to the 2011 maps, are 0.10-0.12 *g* for the 475-year and 0.04-0.06 *g* for the 95-year return period. If we assume deep soil and magnitudes of most contributing earthquakes smaller than 5.5, the PGA values for Osijek are to be multiplied by 1.5 (see Table 1 - Ground Type C and Type 2 Spectrum). As a result, the "final" PGA value for Osijek would be equal to 0.15-0.18 *g* for a 475-year and 0.06-0.09 *g* for a 95-year return period. As shown in Table 2, the empirical PGA estimates based on the intensities provided in the 1990

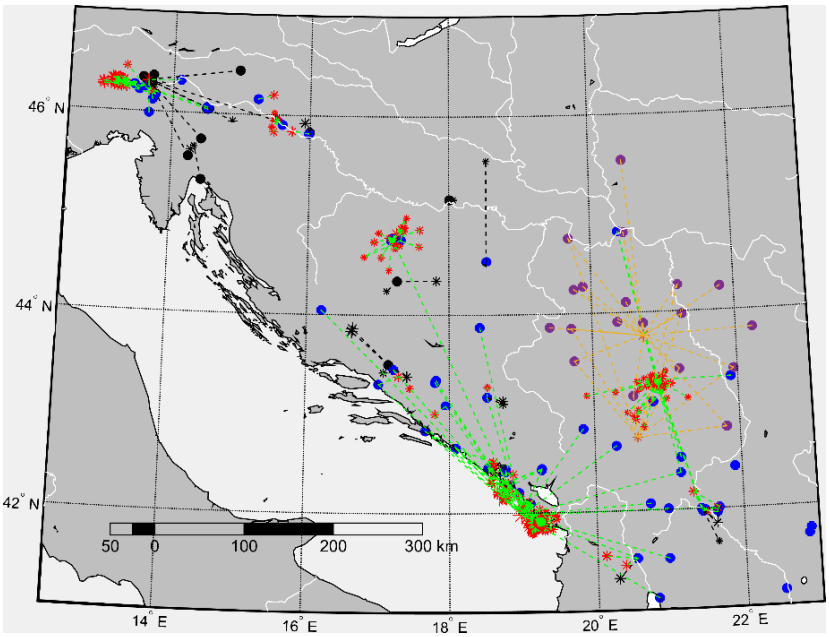

Fig. 3 Map of strong motion records in the north-western Balkans; blue circles and red asterisks represent the EQINFOS (Jordanovski *et al.* 1987) recording locations and earthquakes, respectively; the epicenters are connected to the ground motion stations by green dashed lines; the additional records from the ISESD (Ambraseys *et al.* 2002, 2004) database are represented by black circles, black asterisks, and black dashed lines; the positions of the recording sites and earthquakes for the accelerograms obtained by SSoS (2021) are indicated by violet circles and orange asterisks, respectively

hazard maps are quite similar to the PGA values calculated for Osijek based on the 2011 hazard maps.

2.4 Numerical simulation procedure

The northwestern Balkans are not only a region with hundreds of strong ground motion records but also one of the few regions in the world with data on deep geological conditions for many recording stations.

The regional strong motion data were utilized to create several GMPEs that can account for the effects of local soil (up to depths of 100 m and beyond) and deep geology at the same time (Lee and Trifunac 1993, Lee and Manić 1994, Bulajić *et al.* 2013). The GMPEs were then used in a series of recent microzonation studies (e.g., Lee *et al.* 2015, 2017a, b, c), the results of which were shown to be in great agreement with the observed macroseismic intensities (Bulajić *et al.* 2018, Manić *et al.* 2015).

It is also worth noting that these microzonation studies revealed that PGA amplitudes are dominantly influenced by the local seismicity and are not particularly sensitive to very strong and distant events like those in Romania's Vrancea source zone (Lee *et al.* 2016a, b). This is the case because high-frequency seismic waves attenuate quickly. As a result, when traveling from extremely far away, their final contribution is less than the contribution of the waves caused by local events.

We will now try to generate new regional empirical equations for predicting PGA values that can be applied to deep soil sites and deep geological strata. The attenuation equations will be written in the following mathematical form

$$\log(PGA) = c_1 + c_2 \cdot M + c_3 \cdot log(\sqrt{R^2 + {R_0}^2}) + \\ + c_4 \cdot S_{L1} + c_5 \cdot S_{L2} + c_6 \cdot S_{G1} + c_7 \cdot S_{G2} + \sigma_{log} \cdot \varepsilon \quad (2)$$

where PGA denotes horizontal peak ground accelerations (in g), M the earthquake magnitude (please see Lee *et al.* 1990 for more information on magnitude type), and R the hypocentral or epicentral distance (we will develop equations for each type of distance). S_{L1} and S_{L2} are categorical variables for local soil, and S_{G1} and S_{G2} are categorical variables for deep geological conditions. Table 3 shows the values of these categorical variables.

The database used to create predictive equations contains 436 horizontal components of strong-motion accelerograms recorded from 112 earthquakes with a magnitude of $3 \leq M \leq 6.8$. As the database does not include large magnitude events, the obtained predictive equations will be only applicable for moderate earthquakes. All of the accelerograms were recorded in the north-western Balkans. The majority (418) was recorded between 1976 and 1987 (Jordanovski *et al.* 1987, Ambraseys *et al.* 2002, 2004), with the remainder (18) in 2010.

Fig. 3 depicts a map of regional strong motion records, with full circles representing recording station locations, stars representing earthquake epicenters, and dashed lines connecting epicenters and recording stations.

The MATLAB® scripts for deriving the GMPEs for horizontal PGA values are prepared in version 8.5 release 2015a. We did multiple linear regression analyses in two phases. In the first phase, we fitted Eq. (2) to a strong motion dataset containing only the 406 horizontal acceleration components from the EQINFOS database (Jordanovski *et al.* 1987), for which the soil classification of

Table 3 Categorical variables employed in this study for various types of local soil and deep geological site environments

Local soil parameters	Local soil categorical variables	Deep geology parameters	Deep geology categorical variables
"Rock" soil sites: s_L=0	S_{L1}=S_{L2}=0	Basement (Geological) rock: s=2	S_{G1}=S_{G2}=0
Stiff soil sites: s_L=1	S_{L1}=1 and S_{L2}=0	Intermediate (or complex) sites: s=1	S_{G1}=1 and S_{G2}=0
Deep soil sites: s_L=2	S_{L1}=0 and S_{L2}=1	(Deep geological) Sediments: s=0	S_{G1}=0 and S_{G2}=1

the recording sites was defined by Trifunac *et al.* (1991) and later refined and updated by Lee and Trifunac (1993) and Lee and Manić (1994). We fitted Eq. (2) without the coefficient c_5 because there were no deep soil sites among the 406 components. As a result, we only calculated c_1, c_2, c_3, c_4, c_6, and c_7. To maximize the R^2 statistics of the PGA prediction, the R_0 values were iteratively changed.

Because the majority of the data was collected at shorter distances, we conducted a supplementary analysis utilizing only data collected at epicentral distances of less than 30 km. We calibrated the generated prediction model in the second phase by restricting the coefficient c_5 based on the extra 30 acceleration components recorded at the deep soil sites. The additional data was either included in the ISESD database (Ambraseys *et al.* 2002, 2004) or captured in 2010 by the accelerograph network run by the Seismological Survey of Serbia (SSoS 2021).

For all regression analyses, the analyzed data were assumed to have a log-normal distribution. In Eq. (2), σ_{log} is the standard deviation of the common logarithm of PGA, where ε=0 for the median and ε=1 for the median +1×σ_{log} estimate.

The finalized scaling equations for the horizontal PGA are as follows:

1) based on data collected at all source-to-site distances, the equation with R as the epicentral distance

$$\log(PGA) = -1.2864 + 0.3937 \cdot M - 1.3820 \cdot \log(\sqrt{R^2 + 19.5^2}) + 0.1764 \cdot S_{L1} - 0.0820 \cdot S_{L2} - 0.1498 \cdot S_{G1} - 0.1085 \cdot S_{G2} + 0.2692 \cdot \varepsilon \quad (3)$$

2) based on data collected at all source-to-site distances, the equation with R as the hypocentral distance

$$\log(PGA) = -0.8793 + 0.3730 \cdot M - 1.5096 \cdot \log(\sqrt{R^2 + 25.2^2}) + 0.1961 \cdot S_{L1} - 0.1435 \cdot S_{L2} - 0.1303 \cdot S_{G1} - 0.1066 \cdot S_{G2} + 0.2764 \cdot \varepsilon \quad (4)$$

We also utilized the same coefficients for deep soil sites in equations based solely on data collected at epicentral distances of less than 30 km:

3) using R as the epicentral distance in the equation

$$\log(PGA) = 3.1399 + 0.3864 \cdot M - 3.8132 \cdot \log(\sqrt{R^2 + 40.0^2}) + 0.1015 \cdot S_{L1} - 0.0820 \cdot S_{L2} - 0.2387 \cdot S_{G1} - 0.0893 \cdot S_{G2} + 0.2689 \cdot \varepsilon \quad (5)$$

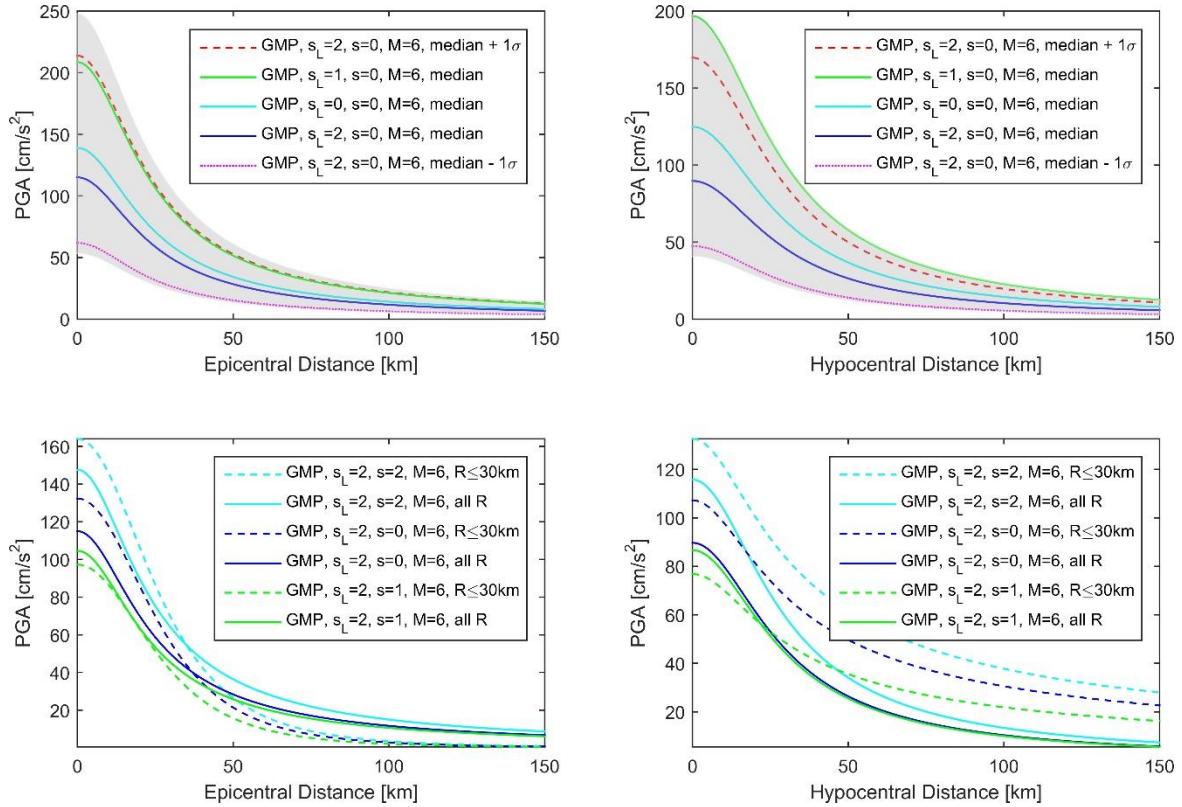

Fig. 4 Empirical GMPE curves for PGA, derived using Eqs. (3)-(6) for various local soil and deep geology conditions (see Table 3)

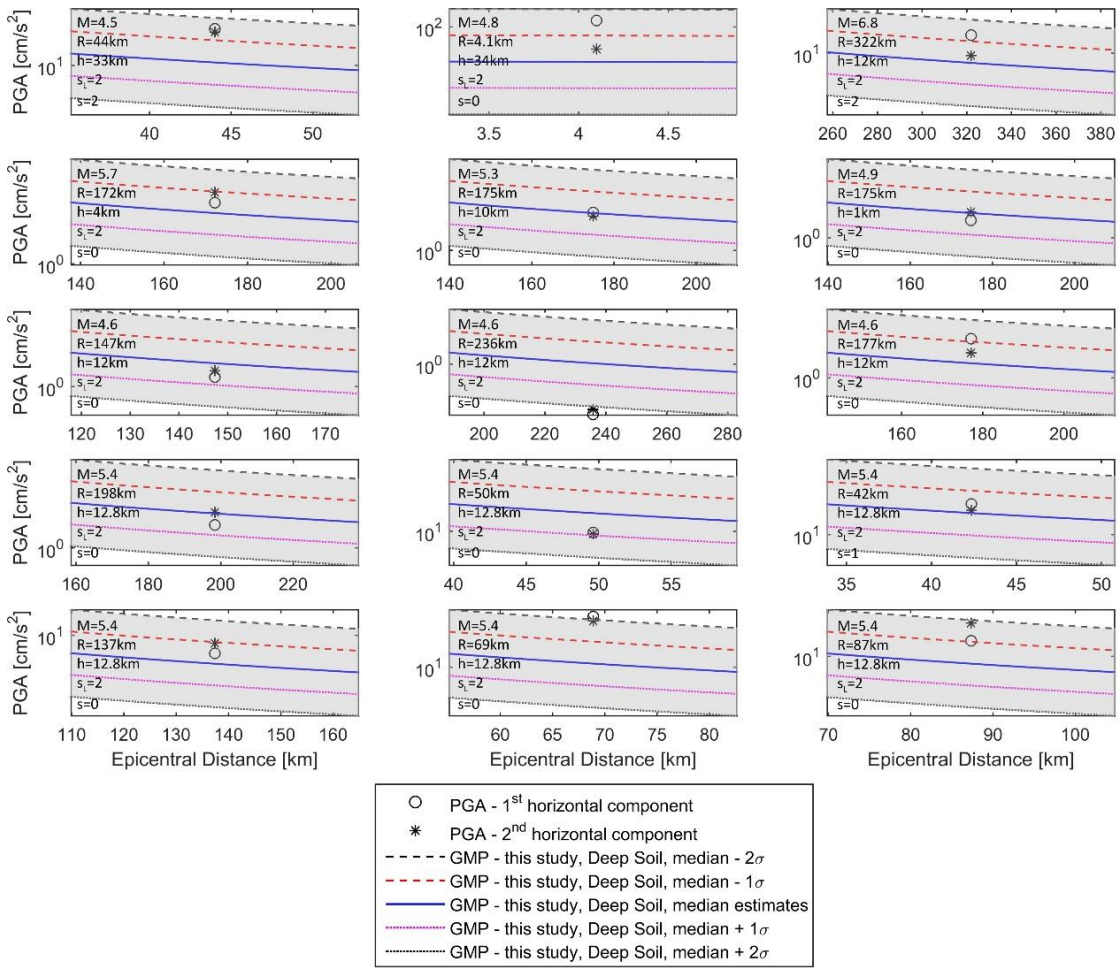

Fig. 5 Comparison of the median, median ±1×σ_{log}, and median ±2×σ_{log} (gray shaded areas) empirical estimates obtained using Eqs. (3) and (5), with recorded PGA values at deep soil sites and different deep geological conditions

4) using R as the hypocentral distance in the equation

$$\log(PGA) = -2.0081 + 0.3698 \cdot M - 0.7030 \cdot \log(\sqrt{R^2 + 18.5^2}) + 0.1044 \cdot S_{L1} - 0.1435 \cdot S_{L2} - 0.2497 \cdot S_{G1} - 0.0884 \cdot S_{G2} + 0.2765 \cdot \varepsilon \quad (6)$$

Fig. 4 depicts the attenuation of PGA as a function of distance, as estimated by Eqs. (3)-(6). The coefficients of the categorical variables S_L and S_G can be used to calculate the differences between values estimated by the same equation and for various site conditions (see Table 3). If the deep geology conditions remain the same and Eq. (3) is used for the epicentral distances and all data, the PGA value for stiff soil sites will be $10^{0.1764}$=1.50 times larger than the PGA for rock soil sites. PGA for deep soil sites will be equal to $10^{-0.0820}$=0.83 times the PGA for rock soil locations using the same equation. To put it another way, horizontal short-period seismic waves at the surface will be de-amplified at deep soil sites compared to the rock sites. This suggests that the energy dissipation of short-period waves in deep soils overcomes a local soil amplification that is caused by the impedance contrast between the deep soil and harder rocks beneath.

Similarly, assuming the local soil conditions remain constant, the PGA estimates at the geological rock will be $1/10^{-0.1085}$=1.28 times larger than at geological sediments, and $1/10^{-0.1498}$=1.41 times larger than at intermediate sites. The fact that short-period waves pass more easily through more compact and harder rock formations (such as basalts and granites) than geological sediments and intermediate geological environments may explain this amplification at geological rock sites.

If empirically defined effects of deep soil sites and deep geological sediments are combined, PGA estimates will be $10^{-0.0820}/10^{-0.1085}$=0.83·1.28=1.06 times larger than at rock soil sites atop geological rocks.

The median, median ±1×σ_{log}, and median ±2×σ_{log} GMPE estimates obtained using Eqs. (3) and (5) are compared to the observed PGA values for the deep soil sites in Fig. 5. The empirical predictions are in excellent agreement with the deep soil PGA values recorded in the region, as shown in Fig. 5.

The presented GMPEs do not consider potential PGA changes as a function of rupture direction relative to the examined site. According to a recent study, the directivity phenomenon (i.e., the existence of high-velocity pulses) can have a major influence on masonry structures like those seen in Osijek (Bilgin and Hysenlliu 2020). Furthermore, near-field and far-field earthquake effects on low-rise buildings like the ones dominating in Osijek are shown to depend on the local soil conditions (Sonmezer and Celiker

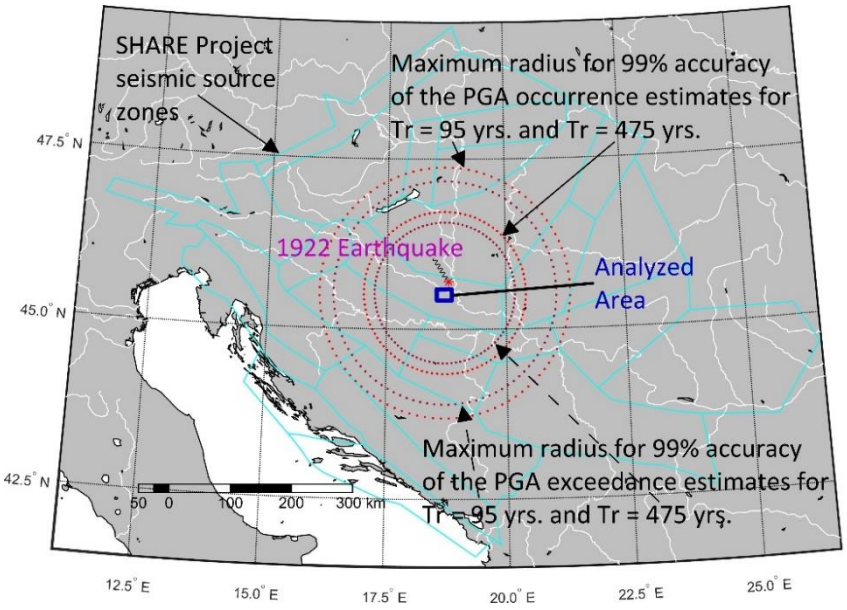

Fig. 6 The SHARE Project seismic source zones (Giardini *et al.* 2013, Wössner *et al.* 2015, Pagani *et al.* 2018) used in this investigation for hazard assessments; the two larger circles, with radii of 182.5 km and 205 km, reflect the distances that must be included in the 95-year return period PSHA calculations for the study area to achieve at least 99 percent and exact 99 percent of the total hazard estimates, respectively; the two smaller circles with radii of 115 km and 132.5 km exhibit the same for the return period of 475 years

2020). However, due to a lack of sufficient directivity and near-field data in regional strong motion records, this will remain beyond the purview of our current study.

In this research, we employed the empirical GMPEs to directly predict deep soil surface response. Though we did not compare our empirical estimates to the modeled soil response using pattern recognition methods (see, for example, Javadi and Rezania 2009) or various equivalent linear and nonlinear analyses (Jakka *et al.* 2015, Onturk *et al.* 2020, Saffarian *et al.* 2014a, b, Sahin 2015a, b, Sonmezer *et al.* 2018), we intend to do so in the future, based on geotechnical data. Because Osijek lacks a dense network of soil profiles, we may need to interpolate available data on soil profiles (see, e.g., Aziz *et al.* 2017) to encompass the whole study area.

3. Results-Seismic microzonation for the case-study area

Assuming deep soil sites and deep geological deposits for the entire case-study area and using Eq. (3) as the GMPE, we have conducted a PSHA analysis for the area within the blue rectangle shown in Fig. 6. The PSHA analysis will be based on Cornell's (1968) and McGuire (1976)'s approach and will follow Chioccarelli *et al.*'s (2019) procedure. The overall hazard within the studied area is the sum of each source zone's contributions, *i* (from the entire set of zones *I*). For all PSHA analyses, we will use the SHARE Project's pan-European seismic source zone model (Giardini *et al.* 2013, Wössner *et al.* 2015, Pagani *et al.* 2018).

The boundaries of the selected seismic source zones for the hazard calculations in this study are shown in Fig. 6. Although it is beyond the focus of this study, the seismic source zones can also be defined using publicly available regional seismological data (Amaro-Mellade *et al.* 2017, 2020, 2021).

To calculate the total hazard, we will apply the so-called law (or formula) of total probability (Ang and Tang 2006), which states that the probability that an event *A* occurs if a series of *n* mutually exclusive events, H_i, occurs, where H_i comprise a full system of hypotheses about the event *A*, is

$$P(A) = \sum_{i=1}^{n} P(A|H_i) \cdot P(H_i) \tag{7}$$

As a result, we use the following formula to compute the mean annual rate of occurrence of seismic events that may cause a PGA to exceed the expected *pga*

$$N(pga) = \sum_{i \in I} \nu_i \int_{M_{min}}^{M_{max}} \int_{R_{min}}^{R_{max}} f_{gmpe}(PGA > pga\,|M,R) \cdot f_{m_i}(M) \cdot f_{r_i|m_i}(R|M) dM dR \tag{8}$$

where *i* is the source zone number (from the set *I*), and *ν* is the yearly rate of earthquakes exceeding $M_{\min}$ and is defined as

$$\nu = e^{a \ln 10 - (b \ln 10) M_{min}} \tag{9}$$

In Eq. (9), *a* and *b* are the Gutenberg and Richter (1944) coefficients, which characterize the overall level of seismicity in the study area and the ratio between small- and large-magnitude events, respectively, and are defined as

$$\log N_{GR}(M) = a - b \cdot M \tag{10}$$

where N_{GR} is the rate of occurrence of events of various magnitudes for each zone *i*. $M_{\max}$ is the greatest regarded magnitude for each zone *i*, $M_{\min}$ is the lowest considered magnitude (although the SHARE seismic-hazard map for

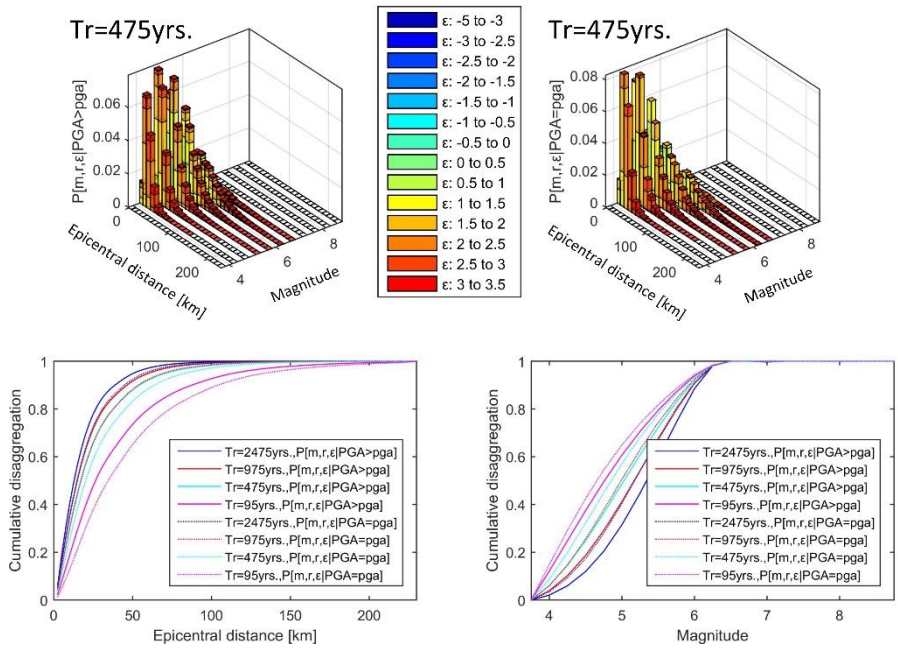

Fig. 7 Top plots-seismic hazard disaggregation for the location 45°32' N, 18° 23' E (see Figs. 8 and 9), return period *Tr*=475 years, and the exceedance and occurrence probabilities; bottom plots-for various return periods, cumulative disaggregated values of epicentral distance and magnitude

entire Europe was calculated with M_{min}=4.5 (Wössner *et al.* 2015), we opted to use M_{min}=4.0 for all zones in this study, to obtain more conservative PGA estimates for smaller return periods), and R_{min} and R_{max} are defined as 0 and 300 km, respectively.

The conditional cumulative distribution function, f_{gmpe}, depends on the GMPE and defines the probability that PGA will exceed *pga* if an event of size *M* occurs at a distance *R*. The probability density function for distance is denoted by $f_{r|m}$, and the probability density function for magnitudes, f_m, is defined as follows

$$f_m(M) = \beta \frac{e^{-\beta(M-M_{min})}}{1-e^{-\beta(M_{max}-M_{min})}}\ ,\ M_{min} \le M \le M_{max}, \quad (11)$$

where β=(ln10)*b*.

The following formula is used to calculate the "return period"

$$Tr = N(pga)^{-1} \quad (12)$$

Although *Tr* is frequently used in engineering literature as an intuitive measure of hazard level (larger *Tr* corresponds to stronger events that occur less frequently, and vice versa), it lacks a unique physical meaning in the sense that it does not (in general) correspond to any single earthquake of engineering interest. This is because the data from all the analyzed seismic source zones are merged and summed over all magnitudes and distances to calculate *N*(*pga*) for a specific location.

If homogeneous Poisson distributions are assumed, the annual probability, i.e., the probability of at least one yearly exceedance of the expectation *pga*, can be calculated as follows (Ang and Tang 2006)

$$P(pga) = 1 - e^{-N(pga)} \quad (13)$$

If a binomial distribution is considered, the probability that *pga* will be exceeded at least once throughout *t* years can be calculated as follows (Ang and Tang 2006)

$$p(pga) = 1 - [1 - P(pga)]^t \quad (14)$$

Table 4 Four alternative seismic hazard probability measures: *P*(*pga*) is the annual probability of minimum one exceedance of the expectation *pga*; *p*(*pga*) represents the probabilities of minimum one exceedance of the expectation *pga* in *t*=10 or 50 years, and *Tr*(*pga*) is the so-called "return period"

$P(pga)$	$p(pga)$ [%] *in t=10 yrs.*	$p(pga)$ [%] *in t=50 yrs.*	$Tr(pga) = \frac{1}{N(pga)} \cong \frac{1}{P(pga)} = \frac{1}{1-\sqrt[t]{1-p(pga)}}$ [yrs.]
0.020000	18.29	63.58	50.00
0.010481	10.00	40.95	95.41
0.005000	4.89	22.17	200.00
0.002105	2.09	10.00	475.06
0.001000	1.00	4.88	1000.00
0.000100	0.10	0.50	10,000.00

Table 4 presents the values of alternative metrics for the level of seismic hazard.

A procedure known as "seismic hazard disaggregation" can be used to determine the most contributing earthquakes to the estimated hazard level (Bazzurro and Cornell 1999). It is effectively the opposite of the process described in Eq. (8), and it allows us to separate independent contributions from distinct pairs of magnitude and distance. As a result, we can specify the number of standard deviations that log(*pga*) is distant from the median empirical estimate for each pair of *M* and *R* (McGuire 1995).

The PSHA disaggregation for the position 45° 32' N, 18° 23' E (see the red circles in Figs. 8 and 9) and *Tr*=475 years are shown in the top plots of Fig. 7. The cumulative

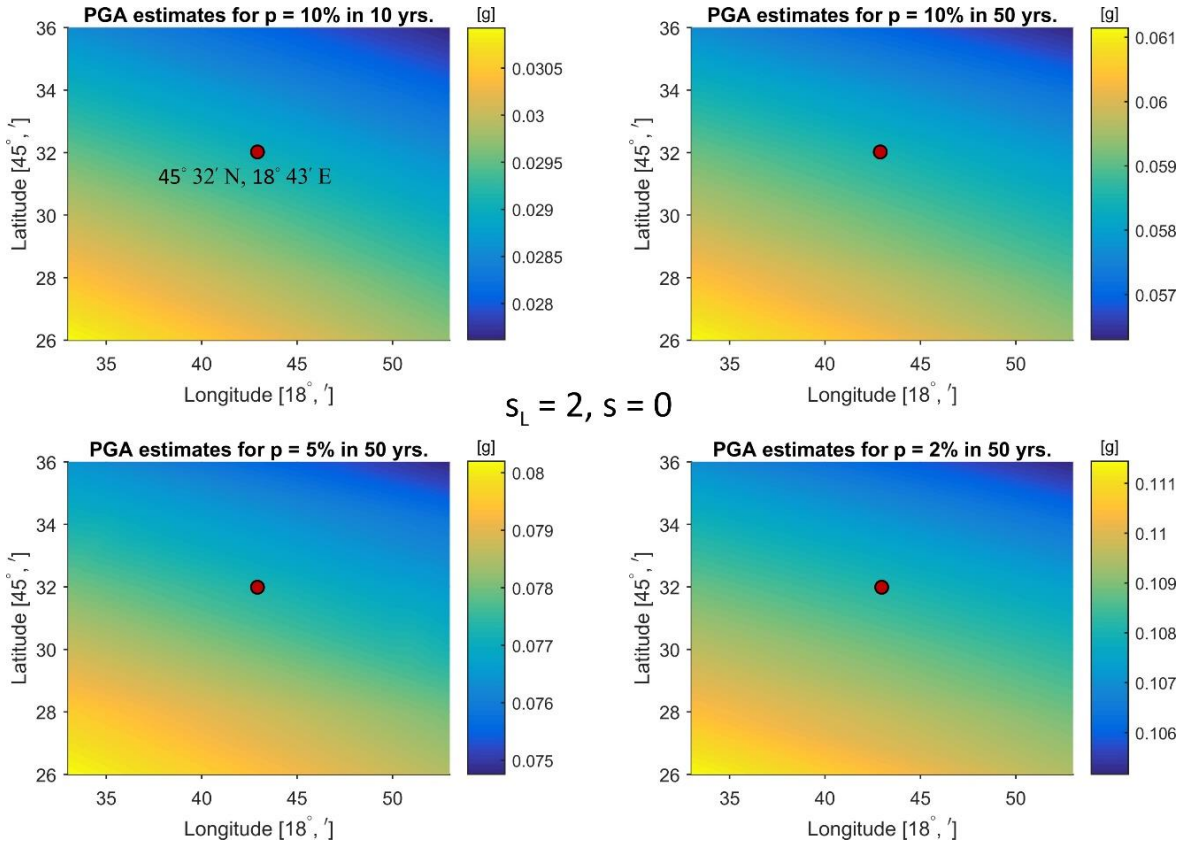

Fig. 8 Seismic microzonation maps for probabilities of p in t years that correspond to return periods of 95 (top left), 475 (top right), 975 (bottom left), and 2475 (bottom right) years, for the deep soil and deep geological sediments; the red circle represents the location for which the hazard was disaggregated, as shown in Fig. 7

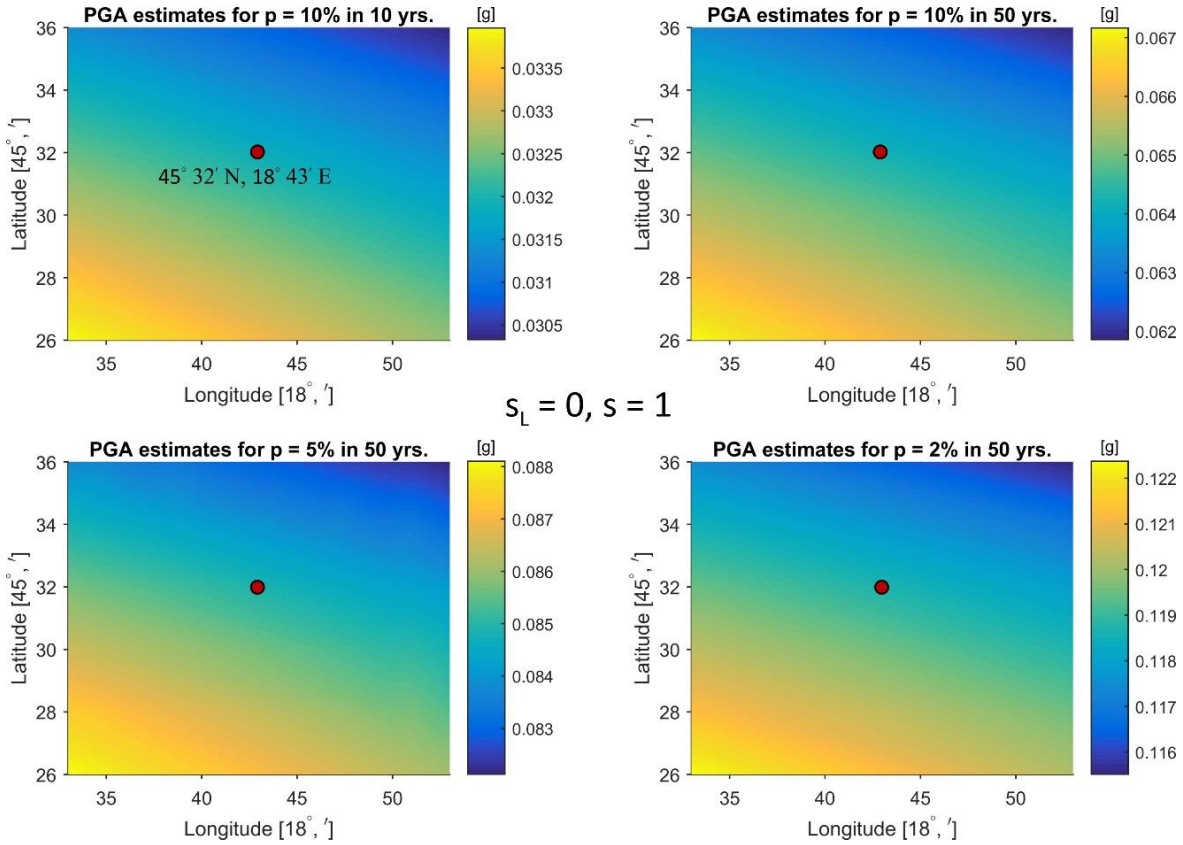

Fig. 9 Seismic microzonation maps for probabilities of p in t years that correspond to the return periods of 95 (top left), 475 (top right), 975 (bottom left), and 2475 (bottom right) years, for the "rock" soil and intermediate deep geology sites

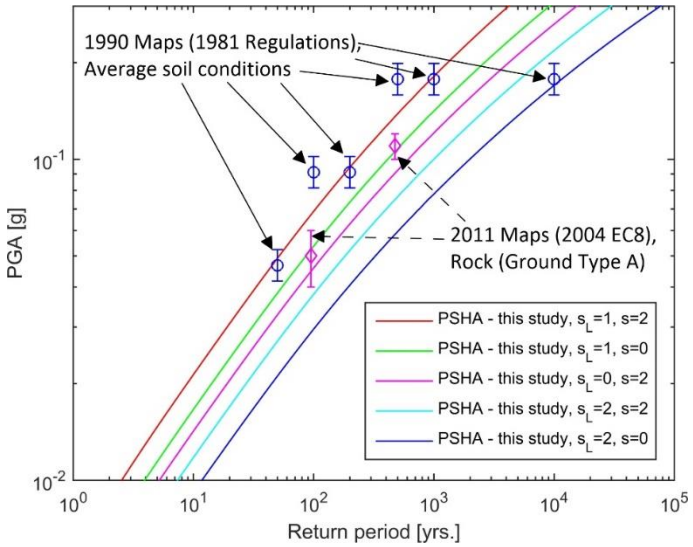

Fig. 10 Comparison of the PGA values defined in this study to the PGA values found in current official Croatian seismic hazard maps (HRN EN 1998-1:2011/NA 2011) and PGA values based on intensity degrees in previous maps (Official Gazette of SFRY 1990); all PGA values are for the position 45° 32' N, 18° 23' E, which is inside the investigated area (see Figs. 8 and 9)

disaggregated values of *R* and *M* are shown in the bottom plots of Fig. 7. For return periods equal to 2475, 975, 475, and 95 years, the bottom left plot in Fig. 7 demonstrates that distances up to, respectively, 15, 15, 17.5, and 27.5 km, contribute to even 50% of the projected probability of exceedance. For the same four return periods, the bottom right plot in Fig. 7 reveals that earthquake magnitudes up to, respectively, 5.5, 5.25, 5.25, and 5.5, contribute to 50% of the projected probability of exceedance.

The maximum epicentral distances that must be included in the PSHA calculations to reach at least 99 percent or exactly 99 percent of the total PGA probability estimates for Osijek are presented by dotted circles in Fig. 6. For example, the circle with a radius of 115 km represents the distances that must be included in the 475-year PSHA calculations to reach at least 99 percent of total hazard estimates. As also shown in Fig. 6, the largest historical earthquake that was reported in Osijek occurred within a 40 km radius of the examined area. The data in Figs. 6 and 7 indicate that, as previously mentioned, the PGA amplitudes are dominated by local seismic activity and are not highly sensitive to the occurrence of distant large earthquakes.

Figs. 8 and 9 show the seismic microzonation maps for the study area. For *Tr*=95, 475, 975, and 2475 years, Fig. 8 displays the first four maps, which were created using Eq. (3) for deep soil locations and deep geological deposits. For the "rock" soil sites and the most prevalent form of deep geology for the recording stations in the region-the intermediate sites (Bulajić *et al.* 2013), "standard" hazard maps were created using Eq. (3). These maps are shown in Fig. 9.

3. Conclusions

In this study, we examine horizontal PGA values in low to medium seismicity regions with deep soil sites atop deep geological sediments. For this reason, Croatia's city of Osijek was chosen as a case study area. With a population of 108,000 inhabitants, Osijek is Croatia's fourth most populous city and the economic center of the region of Slavonia. It has many unreinforced masonry buildings that are sensitive to short-period ground motion (Pavić *et al.* 2020a). The city of Osijek is situated in the Pannonian basin's south-central region, near the rivers Drava and Danube. Underneath the city's local soil, which is categorized as deep soil, are deep geological sediments.

New empirical regional GMPEs for horizontal PGA are presented. The provided equations consider the effects of local soil and deep geological conditions at the same time. According to the new GMPEs, the combination of deep soil and deep geological deposits results in PGA values that are only 6 percent larger than those obtained at rock locations.

Despite the modest number of accelerograms recorded at deep soil sites in the North-Western Balkans and used in this study to calibrate the GMPEs, the empirical estimates are in excellent agreement with both real records and the results of a similar US investigation. As a result, we believe that the data provided here can be utilized as a first step toward defining more trustworthy PGA estimates at deep soil sites in the future, as the number of real ground motion records increases in regions with similar seismic activity and local soil and deep geology properties.

The hazard curves for the position 45° 32' N, 18° 23' E (see Figs. 8 and 9) are compared to the PGA values from Table 2 and the values published in current official Croatian seismic hazard maps (HRN EN 1998-1:2011/NA 2011) to verify the conclusions of our PSHA study, as shown in Fig. 10.

It is worth repeating that the PGA values on the hazard maps included in the National Annex to Eurocode 8 are for "rock or comparable geological formations" (EN 1998-1:2004 2004). Under the former standards, the official

hazard maps were developed for average local soil conditions, and the hazard was estimated using MCS intensity scale degrees (Official Gazette of SFRY 1964, 1982, 1990). The effects of deep geological conditions were not examined in any of these maps.

Furthermore, we conducted additional hazard analyses for the comparisons shown in Fig. 10, using the same Eq. (3) but also considering the deep geological rocks (which can be found in Bansko Brdo hill, only 30 km north of Osijek), as well as the "rock" soil and stiff soil sites, which are presumably also common on the slopes of Bansko Brdo hill. The probabilistic estimates of horizontal PGA values for deep geological rocks and "rock" soil or stiff soil sites are in excellent agreement with the PGA values estimated from macroseismic intensities, and in particularly good agreement with the PGA values given in the 2011 official Croatian maps (HRN EN 1998-1:2011/NA 2011), as shown in Fig. 10. Deep soil hazard estimates, on the other hand, are lower than all the above. The only deep soil PGA estimate that corresponds to the official maps is the one in the 1990 hazard map for a 10,000-year return period.

It is also worth noting that the intensity degrees of VII and VIII °MCS are estimated for the studied area in maps from 1950 (SFRY Official Gazette 1964) and 1982 (SFRY Official Gazette 1982). These intensities correspond to the horizontal PGA values that span the range that includes our estimates for the geological rock beneath "rock" and stiff soil sites.

Even though the hazard curves for the deep soil sites are smaller than all other estimates, we believe the 2011 hazard maps should be used until more data from the deep soil sites is collected and the scaling equations are further assessed and, if necessary, calibrated or modified, especially given the vulnerability of the city of Osijek building stock (Pavić *et al.* 2020a).

References

Amaro-Mellado, J.L. and Tien Bui, D. (2020), "GIS-based mapping of seismic parameters for the pyrenees", *ISPRS Int. J. Geo-Inform.*, **9**(7), 452. https://doi.org/10.3390/ijgi9070452.

Amaro-Mellado, J.L., Melgar-García, L., Rubio-Escudero, C. and Gutiérrez-Avilés, D. (2021), "Generating a seismogenic source zone model for the Pyrenees: A GIS-assisted triclustering approach", *Comput. Geosci.*, **150**, 104736. https://doi.org/10.1016/j.cageo.2021.104736.

Amaro-Mellado, J.L., Morales-Esteban, A., Asencio-Cortés, G. and Martínez-Álvarez, F. (2017), "Comparing seismic parameters for different source zone models in the Iberian Peninsula", *Tectonophys.*, **717**, 449-472. https://doi.org/10.1016/j.tecto.2017.08.032.

Ambraseys, N., Douglas, J., Margaris, B., Sigbjörnsson, R., Berge-Thierry, C., Suhadolc, P., Costa, G. and Smit P. (2004), "Dissemination of European strong-motion data, Volume 2", *Proceedings of the 13th World Conference on Earthquake Engineering*, Vancouver, Canada, August.

Ambraseys, N., Douglas, J., Margaris, B., Sigbjörnsson, R., Smit, P. and Suhadolc, P. (2002), "Internet site for European strong motion data", *Proceedings of the 12th European Conference on Earthquake Engineering*, London, UK, September.

Ang, A.H. and Tang, W.H. (2006), *Probability Concepts in Engineering: Emphasis on Applications to Civil and Environmental Engineering*, John Wiley & Sons, New York, NY, USA.

Aziz, M., Khan, T.A. and Ahmed, T. (2017), "Spatial interpolation of geotechnical data: A case study for Multan City, Pakistan", *Geomech. Eng.*, **13**(3), 475-488. https://doi.org/10.12989/gae.2017.13.3.475.

Balázs, A., Matenco, L., Magyar, I., Horváth, F. and Cloetingh, S. (2016), "The link between tectonics and sedimentation in back-arc basins: New genetic constraints from the analysis of the Pannonian Basin", *Tectonics*, **35**(6), 1526-1559. https://doi.org/10.1002/2015TC004109.

Banak, A., Mandic, O., Sprovieri, M., Lirer, F. and Pavelić, D. (2016), "Stable isotope data from loess malacofauna: Evidence for climate changes in the Pannonian Basin during the Late Pleistocene", *Quat. Int.*, **415**, 15-24. https://doi.org/10.1016/j.quaint.2015.10.102.

Bazzurro, P. and Cornell, C.A. (1999), "Disaggregation of seismic hazard", *Bull. Seismol. Soc. Am.*, **89**, 501-520. https://doi.org/10.1785/BSSA0890020501.

Bielik, M., Makarenko, I., Csicsay, K., Legostaeva, O., Starostenko, V., Savchenko, A., Šimonová, B., Dérerová, J., Fojtíková, L., Pašteka, R. and Vozár, J. (2018), "The refined Moho depth map in the Carpathian-Pannonian region", *Contrib. Geophys. Geodesy*, **48**(2), 179-190. https://doi.org/10.2478/congeo-2018-0007.

Bilgin, H. and Huta, E. (2018), "Earthquake performance assessment of low and mid-rise buildings: Emphasis on URM buildings in Albania", *Eng. Struct.*, **14**(6), 412-427. https://doi.org/10.12989/eas.2018.14.6.599.

Bilgin, H. and Hysenlliu, M. (2020), "Comparison of near and far-fault ground motion effects on low and mid-rise masonry buildings", *J. Build. Eng.*, **30**(3), 101248. https://doi.org/10.1016/j.jobe.2020.101248.

Bilgin, H. and Korini, O. (2012), "Seismic capacity evaluation of unreinforced masonry residential buildings in Albania", *Nat. Hazard. Earth Syst. Sci.*, **12**(12), 3753-3764. https://doi.org/10.5194/nhess-12-3753-2012.

Bulajić, B.Đ., Bajić, S. and Stojnić, N. (2018), "The effects of geological surroundings on earthquake-induced snow avalanche prone areas in the Kopaonik region", *Cold Reg. Sci. Technol.*, **149**, 29-45. https://doi.org/10.1016/j.coldregions.2018.02.005.

Bulajić, B.Đ., Hadzima-Nyarko, M. and Pavić, G. (2021a), "Horizontal UHS amplitudes for regions with deep soil atop deep geological sediments-An example of Osijek, Croatia", *Appl. Sci.*, **11**(14), 6296. https://doi.org/10.3390/app11146296.

Bulajić, B.Đ., Hadzima-Nyarko, M. and Pavić, G. (2021b), "Vertical to horizontal UHS ratios for low to medium seismicity regions with deep soil atop deep geological sediments-An example of the city of Osijek, Croatia", *Appl. Sci.*, **11**(15), 6782. https://doi.org/10.3390/app11156782.

Bulajić, B.Đ., Manić, M.I. and Lađinović, Đ. (2013), "Effects of shallow and deep geology on seismic hazard estimates-A case study of pseudo-acceleration response spectra for the north-western Balkans", *Nat. Hazard.*, **69**(1), 573-588. https://doi.org/10.1007/s11069-013-0726-7.

Bulajić, B.Đ., Pavić, G. and Hadzima-Nyarko, M. (2022), "PGA vertical estimates for deep soils and deep geological sediments-A case study of Osijek (Croatia)", *Comput. Geosci.*, **158**, 104985. https://doi.org/10.1016/j.cageo.2021.104985.

Chioccarelli, E., Cito, P., Iervolino, I. and Giorgio, M. (2019), "REASSESS V2.0: Software for single- and multi-site probabilistic seismic hazard analysis", *Bull. Earthq. Eng.*, **17**(4), 1769-1793. https://doi.org/10.1007/s10518-018-00531-x.

Cornell, C.A. (1968), "Engineering seismic risk analysis", *Bull. Seismol. Soc. Am.*, **58**, 1583-1606. https://doi.org/10.1785/BSSA0580051583.

Douglas, J. (2003), "Earthquake ground motion estimation using strong motion records: A review of equations for the estimation

of peak ground acceleration and response spectral ordinates", *Earth-Sci. Rev.*, **61**, 43-104. https://doi.org/10.1016/S0012-8252(02)00112-5.

EMSC-CSEM (2020) M 5.4-CROATIA-2020-03-22 05:24:02 UTC, European-Mediterranean Seismological Centre (EMSC-CSEM), https://www.emsc-csem.org/Earthquake/earthquake.php?id=840695#scientific.

EN 1998-1:2004 (2004), Design of Structures for Earthquake Resistance, Part 1: General Rules, Seismic Actions and Rules for Buildings, CEN-European Committee for Standardization, Brussels, Belgium.

Ganas, A., Elias, P., Valkaniotis, S., Tsironi, V., Karasante, I. and Briole P. (2021), "Petrinja earthquake moved crust 10 feet", *Temblor.* http://doi.org/10.32858/temblor.156.

Giardini, D., Woessner, J., Danciu, L., Crowley, H., Cotton, F., Grünthal, G., Pinho, R., Valensise, L. and the SHARE Consortium Team (2013), "European Seismic Hazard Map for Peak Ground Acceleration, 10% Exceedance Probabilities in 50 years", The SHARE Consortium.

Gutenberg, B. and Richter, C. (1944), "Frequency of earthquakes in California", *Bull. Seismol. Soc. Am.*, **34**, 185-188. https://doi.org/10.1785/BSSA0340040185.

HRN EN 1998-1:2011/NA:2011 (2011), Eurocode 8, Design of Structures for Earthquake Resistance-Part 1: General Rules, Seismic Actions and Rules for Buildings-National Annex, Hrvatski Zavod za Norme, Zagreb, Croatia.

Inel, M., Ozmen, H.B. and Bilgin, H. (2008), "Re-evaluation of building damage during recent earthquakes in Turkey", *Eng. Struct.*, **30**, 412-427. https://doi.org/10.1016/j.engstruct.2007.04.012.

Işık, E., Büyüksaraç, A., Ekinci, Y.L., Aydın, M.C. and Harirchian, E. (2020), "The effect of site-specific design spectrum on earthquake-building parameters: A case study from the Marmara Region (NW Turkey)", *Appl. Sci.*, **10**, 7247. https://doi.org/10.3390/app10207247.

Işık, E., Kutanis, M. and Bal, I.E. (2016), "Displacement of the buildings according to site-specific earthquake spectra". *Period. Polytech. Civil Eng.*, **60**(1), 37-43. https://doi.org/10.3311/PPci.7661.

Jakka, R.S., Hussain, M. and Sharma, M.L. (2015), "Effects on amplification of strong ground motion due to deep soils", *Geomech. Eng.*, **8**(5), 663-674. https://doi.org/10.12989/gae.2015.8.5.663.

Javadi, A.A. and Rezania, M. (2009), "Applications of artificial intelligence and data mining techniques in soil modeling", *Geomech. Eng.*, **1**(1), 53-74. https://doi.org/10.12989/gae.2009.1.1.053.

Jordanovski, Lj.R., Lee, V.W., Manić, M.I., Olumčeva, T., Sinadnovski, C., Todorovska, M.I. and Trifunac, M.D. (1987), "Strong earthquake ground motion data in EQINFOS: Yugoslavia, Part I", Report No. 87-05, Department of Civil Engineering, University of Southern California, Los Angeles, California, USA.

Kaplan, H., Bilgin, H., Yilmaz, S., Binici, H. and Öztas, A. (2010), "Structural damages of L'Aquila (Italy) earthquake", *Nat. Hazard. Earth Syst. Sci.*, **10**, 499-507. https://doi.org/10.5194/nhess-10-499-2010.

Lee, V.W. (1987), "Influence of local soil and geologic site conditions on Pseudo Relative Velocity spectrum amplitudes of recorded strong motion accelerations", Report No. 87-06, Department of Civil Engineering, University of Southern California, Los Angeles, California, USA.

Lee, V.W. and Manić, M.I. (1994), "Empirical scaling of response spectra in former Yugoslavia", *Proceedings of the 10th Eur. Conf. on Earthq. Eng.*, Vienna, Austria, **4**, 2567-2572.

Lee, V.W. and Trifunac, M.D. (1993), "Empirical scaling of Fourier amplitude spectra in former Yugoslavia", *Eur. Earthq. Eng.*, **7**, 47-61.

Lee, V.W. and Trifunac, M.D. (2010), "Should average shear wave velocity in the top 30 m of soil be the only local site parameter used to describe seismic amplification?", *Soil. Dyn. Earthq. Eng.*, **30**(11), 1250-1258. https://doi.org/10.1016/j.soildyn.2010.05.007.

Lee, V.W., Manić, M.I., Bulajić, B.Đ., Herak, D., Herak, M. and Trifunac, M.D. (2015), "Microzonation of Banja Luka for performance-based earthquake-resistant design", *Soil Dyn. Earthq. Eng.*, **78**, 71-88. https://doi.org/10.1016/j.soildyn.2014.06.035.

Lee, V.W., Trifunac, M.D., Bulajić, B.Đ. and Manić, M.I. (2016a), "A preliminary empirical model for frequency-dependent attenuation of Fourier amplitude spectra in Serbia from the Vrancea earthquakes", *Soil Dyn. Earthq. Eng.*, **83**, 167-179. https://doi.org/10.1016/j.soildyn.2015.12.004.

Lee, V.W., Trifunac, M.D., Bulajić, B.Đ. and Manić, M.I. (2016b), "Preliminary empirical scaling of pseudo relative velocity spectra in Serbia from the Vrancea earthquakes", *Soil Dyn. Earthq. Eng.*, **86**, 41-54. https://doi.org/10.1016/j.soildyn.2016.03.007.

Lee, V.W., Trifunac, M.D., Bulajić, B.Đ., Mani, M.I., Herak, D. and Herak, M. (2017a), "Seismic microzoning of Belgrade", *Soil Dyn. Earthq. Eng.*, **97**, 395-412. https://doi.org/10.1016/j.soildyn.2017.02.002.

Lee, V.W., Trifunac, M.D., Bulajić, B.Đ., Manić, M.I., Herak, D., Herak M. and Dimov, G. (2017b), "Seismic microzoning in Skopje, Macedonia", *Soil Dyn. Earthq. Eng.*, **98**, 166-182. https://doi.org/10.1016/j.soildyn.2017.04.007.

Lee, V.W., Trifunac, M.D., Bulajić, B.Đ., Manić, M.I., Herak, D., Herak, M., Dimov, G. and Gičev, V. (2017c), "Seismic microzoning of Štip in Macedonia", *Soil Dyn. Earthq. Eng*., **98**, 54-66. https://doi.org/10.1016/j.soildyn.2017.04.003.

Lee, V.W., Trifunac, M.D., Herak, M., Živčić, M. and Herak, D. (1990), "M_L^{SM} computed from strong motion accelerograms recorded in Yugoslavia", *Earthq. Eng. Struct. Dyn.*, **19**(8), 1167-1179. https://doi.org/10.1002/eqe.4290190807.

Magaš, N., Mamužić, P., Matičec, D., Prtoljan, B., Galović, I., Sarkotić Šlat, M., Glovacki Jernej, Ž. and Jagačić, T. (1987), "Basic geological map of SFRY-Osijek, L34-86", Geological Institute, Federal Geological Institute of Belgrade, Zagreb.

Manić, M.I., Bulajić, B.Đ. and Trifunac, M.D. (2015), "A note on peak accelerations computed from sliding of objects during the 1969 Banja Luka earthquakes in former Yugoslavia", *Soil Dyn. Earthq. Eng.*, **77**, 164-176. https://doi.org/10.1016/j.soildyn.2015.04.021.

McGuire, R.K. (1976), "Fortran computer program for seismic risk analysis", Technical Report 76-77, US Geological Survey.

McGuire, R.K. (1995), "Probabilistic seismic hazard analysis and design earthquakes: Closing the loop", *Bull. Seismol. Soc. Am.*, **85**(5), 1275-1284. https://doi.org/10.1785/BSSA0850051275.

Morales-Esteban, A., Martinez-Alvarez, F., Scitovski, S. and Scitovski, R. (2014), "A fast partitioning algorithm using adaptive Mahalanobis clustering with application to seismic zoning", *Comput. Geosci.*, **73**, 132-141. https://doi.org/10.1016/j.cageo.2014.09.003.

Morales-Esteban, A., Martinez-Alvarez, F., Scitovski, S. and Scitovski, R. (2021), "Mahalanobis clustering for the determination of incidence-magnitude seismic parameters for the Iberian Peninsula and the Republic of Croatia", *Comput. Geosci.*, **156**, 104873. https://doi.org/10.1016/j.cageo.2021.104873.

Official Gazette of SFRY (1964), Temporary Technical Regulations for Construction in Seismic Areas, Official Gazette of SFRY, 39/64, Belgrade, SFRY.

Official Gazette of SFRY (1982), Book of Rules on Technical Norms for Construction of High-rise Buildings in Seismic Regions, Official Gazette of SFRY, 31/81, 49/82, Belgrade,

SFRY.
Official Gazette of SFRY (1990), Book of Rules on Technical Norms for Construction of High-Rise Buildings in Seismic Regions, Official Gazette of SFRY, 31/81, 49/82, 29/83, 21/88, 52/90.
Onturk, K., Bol, E., Ozocak, A. and Edil, T.B. (2020), "Effect of grain size on the shear strength of unsaturated silty soils", *Geomech. Eng.*, **23**(4), 301-311. https://doi.org/10.12989/gae.2020.23.4.301.
Pagani, M., Garcia-Pelaez, J., Gee, R., Johnson, K., Poggi, V., Styron, R., Weatherill, G., Simionato, M., Viganò, D., Danciu, L. and Monelli, D. (2018), Global Earthquake Model (GEM), Seismic Hazard Map (Version 2018.1 - December 2018).
Pavić, G., Hadzima-Nyarko, M. and Bulajić, B. (2020a), "A contribution to a UHS-based seismic risk assessment in Croatia-A case study for the city of Osijek", *Sustain.*, **12**(5), 1-24. https://doi.org/10.3390/su12051796.
Pavić, G., Hadzima-Nyarko, M., Bulajić, B. and Jurković, Ž. (2020b), "Development of seismic vulnerability and exposure models-A case study of Croatia", *Sustain.*, **12**(3), 1-24. https://doi.org/10.3390/su12030973.
Peng, Y., Wang, Z., Woolery, E.W., Lyu, Y., Carpenter, N.S., Fang, Y. and Huang, S. (2020), "Ground-motion site effect in the Beijing metropolitan area", *Eng. Geol.*, **266**, 105395. https://doi.org/10.1016/j.enggeo.2019.105395.
Pikija, M. and Šikić, K. (1991), "Osnovna geološka karta 1:100.000 list Mohač", Fond Stručnih Dokumenata IGI, Zagreb.
Prelogović, E. and Cvijanović, D. (1981), "Potres u Medvednici 1880. Godine", *Geološki Vjesnik*, **34**, 137-146.
Saffarian, M.A. and Bagheripour, M.H. (2014a), "Seismic response analysis of layered soils considering effect of surcharge mass using HFTD approach. Part I: Basic formulation and linear HFTD", *Geomech. Eng.*, **6**(6), 517-530. https://doi.org/10.12989/gae.2014.6.6.517.
Saffarian, M.A. and Bagheripour, M.H. (2014b), "Seismic response analysis of layered soils considering effect of surcharge mass using HFTD approach. Part II: Nonlinear HFTD and numerical examples", *Geomech. Eng.*, **6**(6). 531-544. https://doi.org/10.12989/gae.2014.6.6.531.
Sahin, A. (2015a), "Dynamic simulation models for seismic behavior of soil systems-Part I: Block diagrams", *Geomech. Eng.*, **9**(2), 145-167. https://doi.org/10.12989/gae.2015.9.2.145.
Sahin, A. (2015b), "Dynamic simulation models for seismic behavior of soil systems-Part II: Solution algorithm and numerical applications", *Geomech. Eng.*, **9**(2), 169-193. https://doi.org/10.12989/gae.2015.9.2.169.
Seed, H.B., Murark, R., Lysmer, J. and Idriss, I.M. (1976b), "Relationships of maximum acceleration, maximum velocity, distance from source, and local site conditions for moderately strong earthquakes", *Bull. Seismol. Soc. Am.*, **66**, 1323-1342. https://doi.org/10.1785/BSSA0660041323.
Seed, H.B., Ugas, C. and Lysmer, J. (1976a), "Site-dependent spectra for earthquake-resistant design", *Bull. Seismol. Soc. Am.*, **66**, 221-243. https://doi.org/10.1785/BSSA0660010221.
Skoko, D., Prelogović, E. and Aljinović, B. (1987), "Geological structure of the Earth's crust above the Moho discontinuity in Yugoslavia", *Geophys. J. R. Astron. Soc.*, **89**, 379-382. https://doi.org/10.1111/j.1365-246X.1987.tb04434.x.
Sonmezer, Y.B. and Celiker, M. (2020), "Determination of seismic hazard and soil response of a critical region in Turkey considering far-field and near-field earthquake effect", *Geomech. Eng.*, **20**(2), 131-146. https://doi.org/10.12989/gae.2020.20.2.131.
Sonmezer, Y.B., Bas, S., Isik, N.S. and Akbas, S.O. (2018), "Linear and nonlinear site response analyses to determine dynamic soil properties of Kirikkale", *Geomech. Eng.*, **16**(4), 435-448. https://doi.org/10.12989/gae.2018.16.4.435.
SSoS (2021), Accelerograms Recorded During March 10, 2010 Peć and November 03, 2010 Kraljevo Earthquakes. Seismological Survey of Serbia (SSoS), Republic of Serbia. http://www.seismo.gov.rs/O%20zavodu/Infol.htm.
Stucchi, M., Rovida, A., Gomez Capera, A., Alexandre, P., Camelbeeck, T., Demircioglu, M.B., ... & Musson, R.M.W. al. (2013), "The SHARE European Earthquake Catalogue (SHEEC) 1000-1899", *J. Seismol.*, **17**, 523-544. https://doi.org/10.1007/s10950-012-9335-2.
Tavakoli, H.R., Amiri, M. T., Abdollahzade, G. and Janalizade, A. (2016), "Site effect microzonation of Babol, Iran", *Geomech. Eng.*, **16**(6), 821-845. https://doi.org/10.12989/gae.2016.11.6.821.
Timkó, M., Kovács, I. and Wéber, Z. (2019), "3D P-wave velocity image beneath the Pannonian Basin using traveltime tomography", *Acta Geodaetica et Geophysica*, **54**, 373-386. https://doi.org/10.1007/s40328-019-00267-3.
Trifunac, M.D. (1990), "How to model amplification of strong earthquake motions by local soil and geologic site conditions", *Earthq. Eng. Struct. Dyn.*, **19**(6), 833-846. https://doi.org/10.1002/eqe.4290190605.
Trifunac, M.D. and Brady, A.G. (1975), "On the correlation of seismic intensity scales with the peaks of recording strong ground motion", *Bull. Seismol. Soc. Am.*, **65**, 139-162. https://doi.org/10.1785/BSSA0650010139.
Trifunac, M.D., Lee, V.W., Živčić, M. and Manić, M.I. (1991), "On the correlation of Mercalli-Cancani-Sieberg intensity scale in Yugoslavia with the peaks of recorded strong earthquake ground motion", *Eur. Earthq. Eng.*, **5**, 27-33. https://doi.org/10.1785/BSSA0650010139.
UNESCO (1974), Catalogue of Earthquakes, Part I, 1901-1970, Part II, Prior to 1901, UNDP/UNESCO Survey of the Seismicity of the Balkan Region, Eds: Schebalin, N.V., Karnik, V., Hadžievski, D., UNESCO, Skopje.
USGS (2017), Earthquake Catalog for all Earthquakes with $M_w \geq 2.5$ in the Period 1900-2017 for the Geographic Region between 40.5° N and 47.5° N, and 12.5° E and 24.5° E. https://earthquake.usgs.gov/earthquakes/search/, last accessed on February 23, 2017.
Woessner, J., Laurentiu, D., Giardini, D., Crowley, H., Cotton, F., Grünthal, G., ... & Stucchi, M. (2015), "The 2013 European Seismic Hazard Model: key components and results", *Bull. Earthq. Eng.*, **13**(12), 3553-3596. https://doi.org/10.1007/s10518-015-9795-1.

CC